MAUSAM, **77**, 3 (July 2026), 1069-1078

MAUSAM

DOI: https://doi.org/10.54302/mausam.v77i3.6802
Homepage: https://mausamjournal.imd.gov.in/index.php/MAUSAM

UDC No.551.576.1:551.577.1:551.508.7

Assessing the Influence of Coalescence on Precipitation Patterns: A Comparative Study with Disdrometer Data

[1]NITA H. SHAH, [2*]JYOTI CHAHAL AND [3]BIPASHA PAUL SHUKLA

[1]*Department of Mathematics, Gujarat University, Ahmedabad-380009, India*

[2]*Center for Professional Courses, Gujarat University, Ahmedabad-380009, India*

[3]*Environment Sciences Division, Space Applications Centre, ISRO, Ahmedabad-380015*

Gujarat, India

E-mail:[1]*nitahshah@gmail.com*, [2]*jyotichahall.jc@gmail.com*, [2]*bipasha@sac.isro.gov.in*,

(*Received 12 August 2024, Accepted 15 April 2025*)

***Corresponding author's email: jyotichahall.jc@gmail.com**

सार – संघनन (Nucleation), द्रवीकरण (Condensation), वाष्पीकरण (Evaporation) और सम्मिश्रण (Coalescence) जैसी सूक्ष्म-भौतिक प्रक्रियाएं वर्षण (Precipitation/बारिश) के निर्माण में केंद्रीय भूमिका निभाती हैं। हालांकि, इन प्रक्रियाओं की जटिल और अत्यधिक परिवर्तनशील प्रकृति के कारण संख्यात्मक मौसम पूर्वानुमान मॉडलों (NWP) में इनका प्राचलीकरण (Parameterization) अनिश्चितता का एक बड़ा स्रोत है। उष्ण मेघ (Warm clouds), जो हिमांक से ऊपर के तापमान द्वारा अभिलक्षित होते हैं, टकराव-सम्मिश्रण (Collision-coalescence) जैसी प्रक्रियाओं के माध्यम से वर्षण उत्पन्न करने में महत्वपूर्ण भूमिका निभाते हैं। इस अध्ययन में, हम सुपर ड्रॉपलेट मॉडल (PySDM) के लिए पायथन फ्रेमवर्क के भीतर क्रियान्वित एक स्टोकेस्टिक सम्मिश्रण मॉडल (Stochastic Coalescence Model - SCM) का उपयोग करके उष्ण वर्षा की सम्मिश्रण गतिकी का अन्वेषण करते हैं। हमने मॉडल के परिणामों को सत्यापित करने के लिए RD-80 इम्पैक्ट डिस्ट्रोमीटर (Impact Disdrometer) डेटा का उपयोग किया, जो वर्षा की बूंदों के आकार के वितरण और वर्षा की विशेषताओं के बारे में अंतर्दृष्टि प्रदान करता है। डिस्ट्रोमीटर से हमारा तात्पर्य एक ऐसे उपकरण से है जिसका उपयोग वर्षण कणों के आकार और वेग को मापने के लिए किया जाता है, जो वर्षण गतिकी को समझने के लिए मूल्यवान डेटा प्रदान करता है। हमारे प्रयोगात्मक सेटअप में एक निर्दिष्ट सम्मिश्रण सेल के भीतर सुपर ड्रॉपलेट्स की सम्मिश्रण प्रक्रिया का अनुकरण (Simulation) करना और परिणामस्वरूप प्राप्त द्रव्यमान घनत्व (Mass density) डेटा की जमीनी अवलोकनों के साथ तुलना करना शामिल था। 20,000 सेकंड की अवधि में फैले 200 प्रयोगों का संचालन करके, हमने ड्रॉपलेट आबादी के क्रमिक विकास को दर्ज किया। हमारे निष्कर्ष धरातलीय मापों और वायुमंडलीय ड्रॉपलेट गतिकी के बीच के अवलोकन संबंधी अंतर को पाटने में PySDM की उपयोगिता को प्रदर्शित करते हैं, जिससे उष्ण वर्षा प्रक्रियाओं की हमारी समझ बढ़ती है और वर्षण पूर्वानुमान क्षमताओं में सुधार होता है।

ABSTRACT. The microphysical processes like nucleation, condensation, evaporation and coalescence are pivotal in precipitation formation. However, the parameterization of these processes are a major source of uncertainty in numerical weather prediction models (NWP) due to their complex and highly variable nature. Warm clouds, characterized by temperatures above freezing, play a significant role in precipitation generation through processes like collision-coalescence. In this study, we explore the coalescence dynamics of warm rain using a stochastic coalescence model (SCM) implemented within the Python framework for the super droplet model (PySDM). We utilized RD-80 Impact Disdrometer data to validate the model results, which provide insights into raindrop size distributions and rainfall characteristics. By Disdrometer, we mean an instrument used to measure the size and velocity of precipitation particles, providing valuable data for understanding precipitation dynamics. Our experimental setup involved simulating the coalescence process of super droplets within a designated coalescence cell and comparing the resulting mass density data with ground observations. By conducting 200 experiments spanning a duration of 20,000 seconds, we captured the evolution of droplet populations. Our findings demonstrate the utility of PySDM in bridging the observational gap between ground-level measurements and atmospheric droplet dynamics, thereby enhancing our understanding of warm rain processes and improving precipitation forecasting capabilities.

Keywords – Super droplet method, Disdrometer, Cloud microphysics, Monte-Carlo simulation, Coalescence

1. Introduction

In the dynamic world of atmospheric processes, warm clouds, characterized by temperatures above freezing, play a pivotal role in the formation of precipitation. Within these clouds, tiny water droplets have the potential to undergo a remarkable transformation. Through a process known as collision-coalescence, they merge to create larger drizzle droplets or raindrops, ranging from a few hundred micrometers to several millimeters in diameter. This meteorological phenomenon, often referred to as "warm rain," stands as a significant contributor to the planet's total precipitation. Notably, it accounts for approximately 30% of the Earth's overall rainfall and holds a dominant presence, contributing to roughly 70% of the total rain area within the tropical regions (Lau & Wu, 2003). The rapid development of larger droplets is a common occurrence within maritime clouds. In contrast, for clouds characteristic of continental climates, it has been established that the coalescence mechanism, essential for raindrop formation, necessitates droplets with a radius exceeding approximately 22μ (Bartlett, J. T. (1966)). Cloud droplets with radii smaller than 10 to 15 μm effectively enlarge as a result of water vapor diffusion, while droplets exceeding 30 to 50 μm in radius efficiently increase in size through gravitational collisions (Beard and Ochs III, 1993; Pruppacher *et al.*, 1998). Radar assessments conducted in tropical areas reveal that the warm rain process can generate precipitation within cumulus clouds in roughly 15 to 20 minutes (Szumowski *et al.*, 1997; Knight *et al.*, 2002; Rogers and Yau, 1989). In the atmosphere, microphysics plays a crucial role in shaping cloud and precipitation particles, dictating their growth via condensation, evaporation, and melting. Given the immense number of particles present, even in a small cloud, it's impractical to simulate each one individually. Instead, atmospheric models utilize statistical approaches to capture the overall evolution of particle populations (Morrison *et.al.* 2020).

Recent advancements in stochastic modeling for precipitation focus on improving rainfall variability representation through high-resolution simulations and data-driven parameter estimation. Modern stochastic models integrate machine learning techniques, such as Bayesian inference and Gaussian processes, to enhance parameter calibration and uncertainty quantification (Onof & Arnbjerg-Nielsen, 2009; Northrop, P. J., 2024). Additionally, stochastic-mechanistic models now incorporate non-stationary processes to better account for seasonal and climate-driven changes in rainfall patterns, improving short-term rainfall predictions and hydrological modeling. Machine learning has further contributed to atmospheric modeling, with deep learning methods like convolutional neural networks (CNNs) and generative adversarial networks (GANs) refining rainfall predictions by leveraging large observational datasets, including disdrometer and radar measurements (Kumar and Sharma, 2025; Zhang *et al.*, 2025; Ma *et al.*, 2024). Furthermore, ensemble machine learning models have improved predictions of complex atmospheric processes, as demonstrated in recent fog prediction studies, where deep learning and distributed random forests effectively captured microphysical variations to enhance visibility forecasting (Shankar, A., 2024). These advancements are particularly relevant to precipitation modeling, where understanding microphysical processes—such as droplet growth, coalescence, and dissipation—is crucial for improving forecasting accuracy. While our study focuses on warm rain processes using PySDM, the insights gained from droplet microphysics contribute to refining machine learning-based precipitation models. Integrating observational microphysics with advanced computational techniques presents a promising direction for future research in rainfall modeling and prediction

2. Data and methodology

2.1. *Model Used*

In collision-coalescence systems, researchers commonly rely on mean-field equations like Smoluchowski's coagulation equation (Smoluchowski's, 1918) to depict the changes in droplet populations over time. This equation describes how droplet distributions evolve due to the interplay of collisions and coalescence events.

$$\frac{dN_m}{dt} = \frac{1}{2}\sum_{k=1}^{m-1} C_{k,m-k} N_k N_{k,m-k} - N_m \sum_{k=1}^{m-1} C_{m,k} N_k \quad (1)$$

Here, N_m represents the mean density of droplets with a mass equivalent to 'm' elemental mass units per unit volume at time 't.' $C_{m,k}$ denotes the collision kernel governing interactions between droplets of 'm' and 'k' sizes. The first component on the right-hand side represents the rate at which m-sized droplets are generated through coalescence events involving pairs of smaller droplets whose combined masses match that of an m-sized droplet. The second component on the right-hand side accounts for the rate of reduction resulting from coalescence events that involve m-sized droplets. This deterministic equation, known as the Smoluchowski's equation or the kinetic collection equation (KCE) (Wang *et. al.*, 2006).

Python framework for the super droplet model (PySDM), is built upon the principles of Smoluchowski's

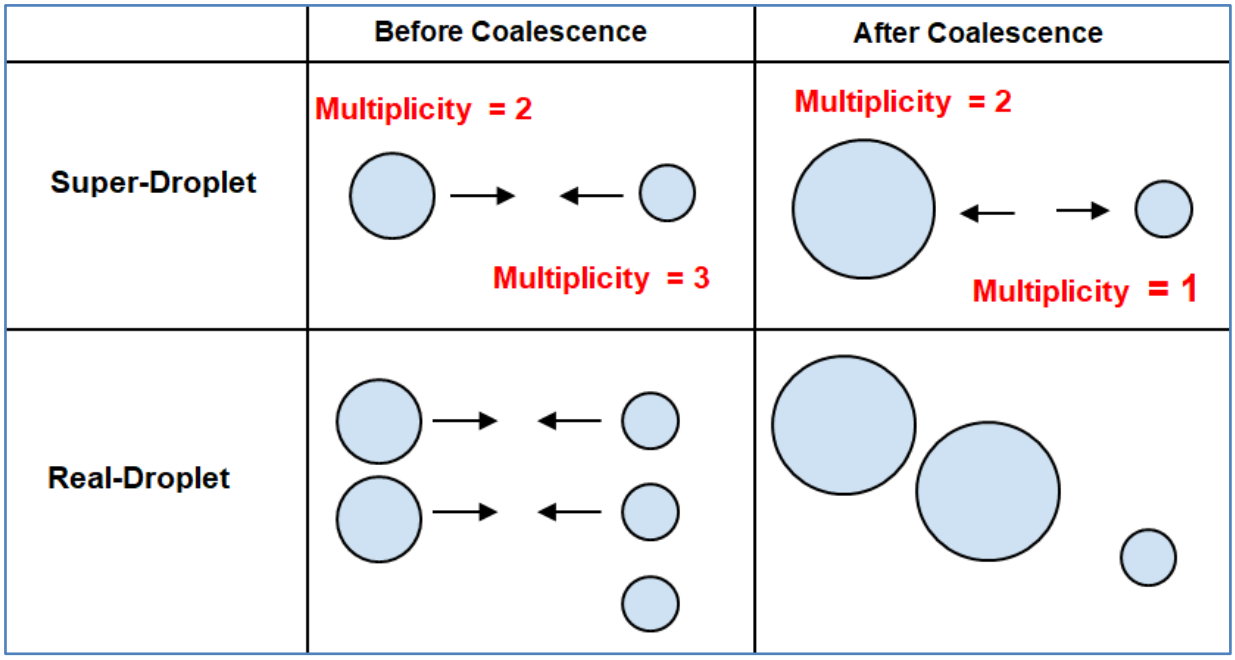

Fig. 1. Coalescence of Super droplets (Shima et.al. 2009)

with accuracy (Bartman, P., & Arabas, S. (2021)). The concept of stochastic coalescence model (SCM) in the field of cloud physics was initially introduced by Telford (1955). This model is founded on stochastic coalescence evolution (SCE) principles, which are instrumental in examining the temporal growth of cloud droplets. The analysis of SCM involved the construction of a function denoted as P (n, m, t), representing the count of 'm' molecules at time't,' which, in turn, signifies the number of cloud drops. The evolution of P (n, m, t) over time was a central aspect of this investigation (Gillespie, 1972). Furthermore, among various influencing factors, the drop size distribution (DSD) is a significant contributor to these dynamics (Gebauer *et al.*, 2006).

2.2 *Stochastic Coalescence of Super Droplet*

Each super-droplet embodies a multitude of individual droplets sharing identical attributes and positions, with the number of constituent droplets represented by the positive integer. This multiplicity varies across super-droplets and evolves over time due to coalescence dynamics. Consequently, each super-droplet possesses its unique position and attributes, characterizing the identical droplets encapsulated within. In the context of warm-rain model, these attributes typically include the equivalent radius of water and the mass of solute, denoted as

$$a_i(t) = [R_i(t), M_i(t)]$$

Fig. 1 illustrating the coalescence process of super-droplets. In the upper left panel, two super-droplets with multiplicities of 2 and 3 respectively, undergo coalescence. This coalescence represents the merging of two pairs of droplets, as depicted in the lower panels. Consequently, the super-droplet with a multiplicity of 2 increases in size, while the multiplicity of the other super-droplet decreases from 3 to 1, as shown in the upper right panel (Shima *et.al.*,2009, Bartman *et al.*, 2021).

2.3. *Data Used*

In this study we used RD-80 Impact Disdrometer data, Disdrometer is a scientific instrument used to measure the size and velocity of precipitation particles falling to the ground. It provides data that helps in understanding the characteristics of precipitation, such as raindrop size distribution, rainfall rate, and rainfall intensity. One common type is the optical disdrometer, which utilizes optical sensors like lasers or infrared beams to detect particles passing through its sensing area. By analyzing the scattering or blocking of light by the particles, optical disdrometer determine both the size and velocity of individual particles. Another type, acoustic disdrometer, relies on sound waves to detect and characterize precipitation particles. These instruments analyze the acoustic signals generated by particle impacts to estimate particle size and velocity, making them particularly useful for measuring snowfall and hail. Impact disdrometer, on the other hand, utilize the

TABLE 1

Radius bins for RD-80 Disdrometer (Bartholomew 2009)

Classes	Radius bins (mm)	Classes	Radius bins (mm)
Class 1	156.5-202.5	Class 11	874.0-1038.5
Class 2	202.5-252.5	Class 12	1038.5-1205.0
Class 3	252.5-298.0	Class 13	1220.5-1363.5
Class 4	298.0-357.5	Class 14	1363.5-1505.5
Class 5	357.5-413.5	Class 15	1505.5-1692.5
Class 6	413.5-499.5	Class 16	1692.5-1852.0
Class 7	499.5-616.0	Class 17	1852.0-2063.5
Class 8	616.0-714.5	Class 18	2063.5-2286.5
Class 9	714.5-791.0	Class 19	2286.5-2572.5
Class 10	791.0-874.0	Class 20	2572.5-2800.25

coagulation equation. This approach is advantageous as it doesn't operate on individual droplets but rather on collections of droplets with similar attributes, known as super droplets. Super droplets facilitate a Monte Carlo-inspired probabilistic modeling approach, offering an efficient means to simulate particle coagulation processes principle of particle impact to measure precipitation. They feature a collection surface or array of sensors that detect particle impacts, allowing for the estimation of particle size and velocity. (Bartholomew, 2009).

The RD-80 disdrometer predefined classifications are presented in millimeters, specifically concerning diameters. To incorporate these classifications into the drop size distribution for PySDM, we conducted a conversion procedure. This involved converting the 20 radius bins from millimeters to micrometers. The resulting converted radius bins are detailed in the table 1.

2.4 *Methodology*

In this investigation, we employed the Rd-80 Disdrometer radius bin (Table 1) as an input parameter in the PySDM model. We recorded the mass density of droplets to analyze their evolution under the coalescence process within a designated coalescence cell. The motivation behind utilizing the Disdrometer bin in PySDM is to facilitate an understanding of the microphysics of droplets. This approach serves to bridge the observational gap between ground-level observations and droplets present in any atmosphere.

2.5 *Experimental Setup*

(i) Select Coalescence cell with a volume $\Delta V = 10^6 m^3$. Initially, the number density of super droplets is $N_s = 2^{15} m^{-3}$Additionally, the initial size distribution of the droplets conforms to an exponential distribution of droplet volumeX_i, denoted by

$$p(X_i) = (\tfrac{1}{X_0})\, exp(-X_i/X_0), X_0 = (4\pi/3)R_0^3, R_0 = 30.531 \times 10^{-6} m \quad (2)$$

(ii) Through the stochastic coalescence of super droplets, all variables undergo updates as prescribed by the principles of super droplet theory (Shima et.al. 2009). Subsequently, we capture the values of the mass density of super droplets using the kernel density estimation method with a Gaussian kernel, the estimator function is defined by

$$g(ln\, R) = \tfrac{1}{\Delta V}\textstyle\sum_{i=1}^{N_s} \xi_i m_i W_\sigma(ln\, R - ln\, R_i), W_\sigma(Y) = \tfrac{1}{\sqrt{2\pi}\sigma} exp(-Y^2/2\sigma^2). \quad (3)$$

Here, ΔV is the volume of the coalescence cell, and $\sigma = \sigma_0 {N_s}^{-1/5}$ with some constant$\sigma_0 = 0.62$.

(iii) PySDM incorporates a Monte Carlo scheme, introducing randomness in the coalescence process of super droplet pairs. To account for this inherent randomness, we conducted 200 experiments within PySDM. Each experiment spanned a duration of 20,000 seconds, with a minute gap between measurements. By specifying the radius bin size of the Disdrometer (Table 1) in PySDM.

(iv) PySDM divides each specific bin into 49 sub-bins and computes the mass density for each of the resulting 49 droplet sizes. Thus, across a total of 20 bins, we have 980 droplet sizes, with the corresponding mass density data stored for 200 experiments. For comparison with

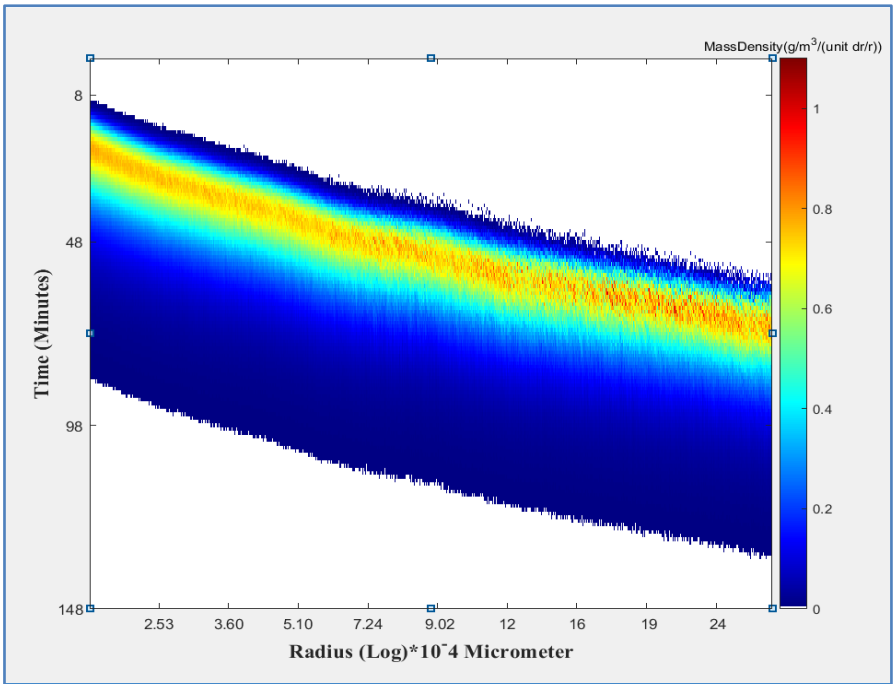

Fig. 2. Temporal evolution of droplets of Disdrometer Radius bin range (156.5-2800.25) micrometers

Disdrometer data, we compute the average mass density for the first 49 droplets, then proceed similarly for subsequent sets of 49 droplets, corresponding to the 20 Disdrometer bins.

(v) To compare the ground observations with the observed values through PySDM we fileted the Disdrometer data and obtained the continuous rainfall data for 150 minutes in which rain rate (R (mm/h) > 10) which we took for Ahmedabad 2005 august data as 2005 is the flood year for Ahmedabad and converted the number of droplets into mass density data by formulae

$$\text{M D } (g/m^3) = (\text{N} \times \text{V} \times \text{D}) \times 1000, \qquad (4)$$

where, MD is the mass density of droplets, N is the number of droplets, V represents the volume of each droplet and D represents the density of water. The volume of each droplet was calculated using the formula for the volume of a sphere: $4/3 * \pi R^3$, Where, R radius of droplet is known.

3. Results and discussion

The coalescence in the droplets is influenced by many factors: droplet size, temperature, relative humidity, updrafts and downdrafts but one major factor is the size of droplets. The evolution of drop size distribution over time is primarily governed by rates of drop breakage and coalescence, which are inherently dependent on the sizes of the drops themselves (Kopriwa *et.al.* 2012).

Fig. 2 illustrates the variation of droplet mass density with radius and time. The maximum mass density, represented by the red regions, occurs at different times for different droplet radii. Notably, larger droplets reach their peak mass density much later than smaller ones. This behavior is more clearly visualized in Figs. 3 and 4.

Fig. 3 illustrates the density distribution of droplets within each size bin, following a Gaussian-like pattern**.** This distribution suggests that within any given size range, most droplets cluster around a central mass density, while fewer exist at the extremes. However, the timing of this distribution varies across different bins, as depicted in Figs. 4 (a & b).

In real-world scenarios, this behavior plays a crucial role in rainfall formation, cloud microphysics, and weather prediction. During the early stages of cloud development, small droplets dominate, undergoing rapid coalescence**,** which leads to an increase in their size and mass density (Pruppacher & Klett, 1998). As this process continues, droplets grow and shift into larger size bins, causing the peak mass density to move progressively toward higher droplet sizes. This phase is critical for precipitation initiation, as larger droplets have a higher probability of falling as raindrops (Beard & Ochs, 1993). However, beyond this peak, other microphysical processes come into play. One such process is the breakup, where larger droplets collide with sufficient force, causing them to split into smaller fragments (Ko & Ryou, 2005). These smaller fragments contribute to a reduction in mass

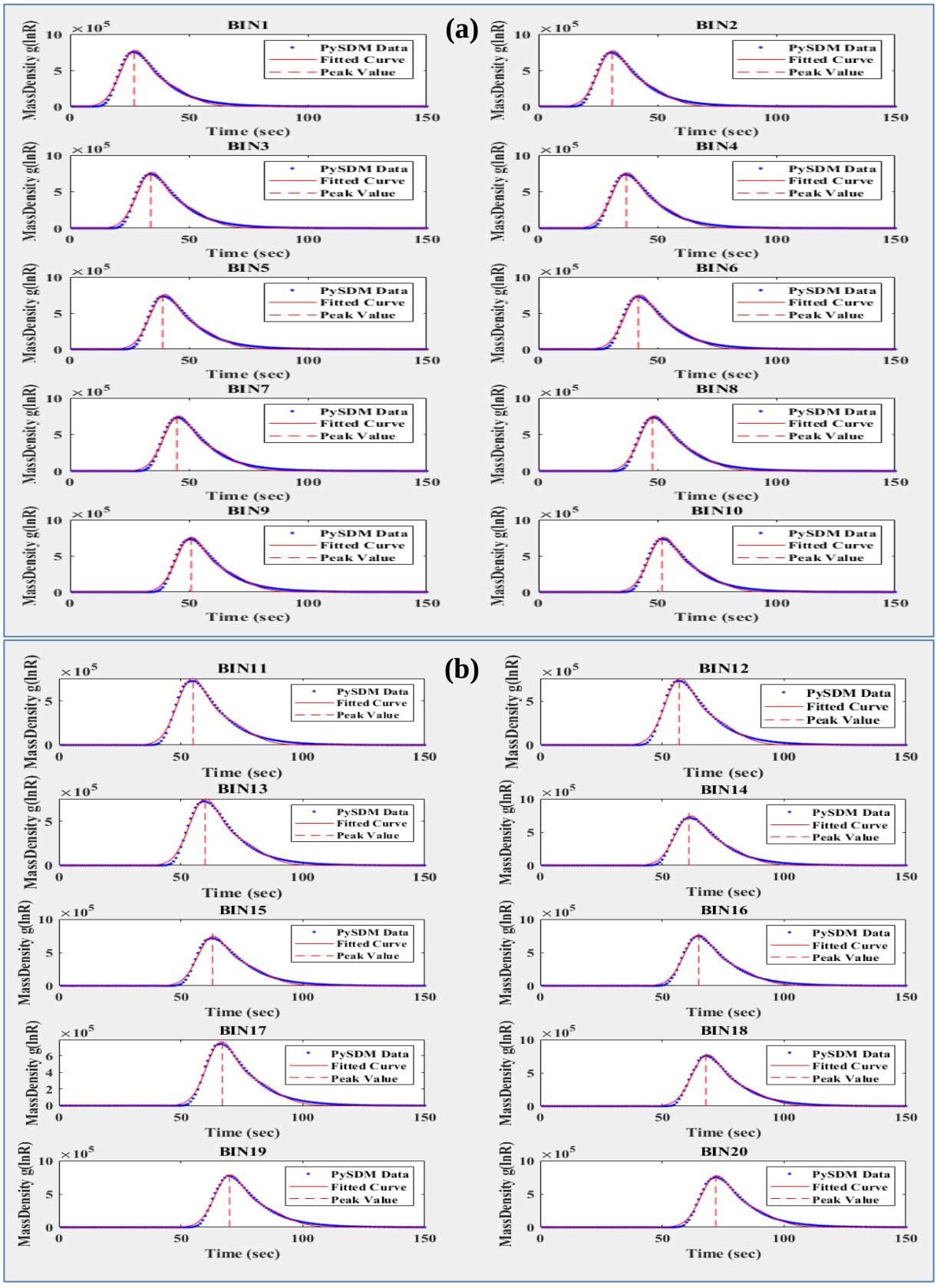

Figs. 3(a&b). a) Temporal variation of mass density for Bin 1- Bin 10. b) Temporal variation of mass density for Bin10-Bin20

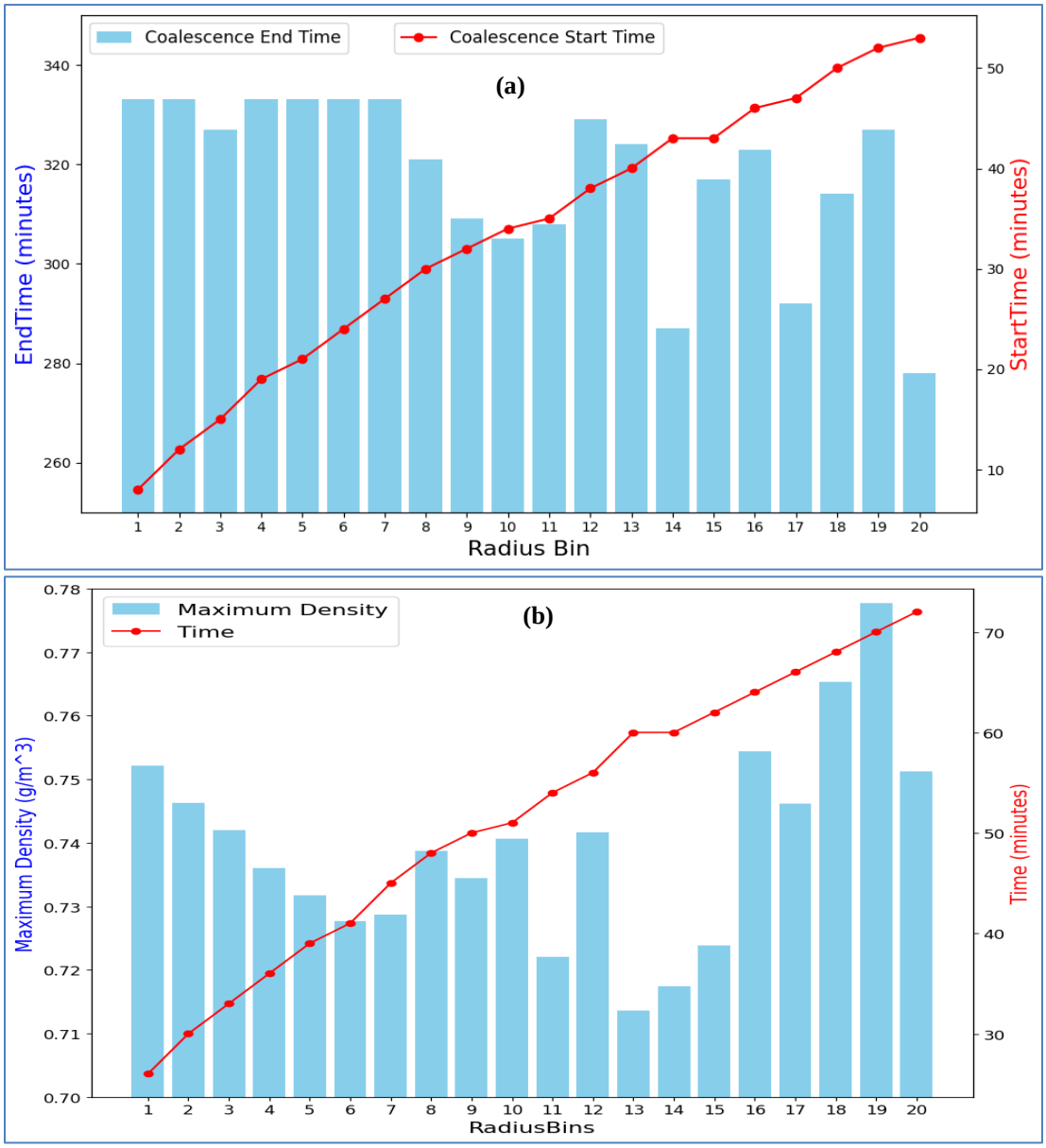

Fig. 4 (a&b). a) Time for initiation and cessation of coalescence in each bin. b) The maximum density of droplets observed within each radius bin, alongside the corresponding time at which this maximum density is achieved

density within the size bin as they disperse across smaller categories. Thus, the transition from the dominant coalescence stage to the breakup stage marks a shift in the dynamics of droplet interactions, ultimately influencing the mass density distribution within the size bin.

This shift between size bins has practical applications in weather forecasting, radar-based rainfall estimation, and cloud modeling. In convective storms, strong updrafts sustain smaller droplets in the cloud for longer durations, allowing for extended coalescence and larger raindrop formation, leading to heavy rainfall events. Conversely, in arid regions, rapid evaporation and weaker coalescence result in smaller, short-lived raindrops, affecting rainfall efficiency. Understanding how droplets change size and shift between bins helps improve satellite-based precipitation retrieval algorithms, which rely on accurate droplet size distributions for estimating rainfall rates (Seifert, A., et.al., 2005). Recognizing the transition from coalescence-dominated growth to fragmentation provides insights into cloud lifetime and precipitation efficiency, contributing to improved weather prediction and climate modeling.

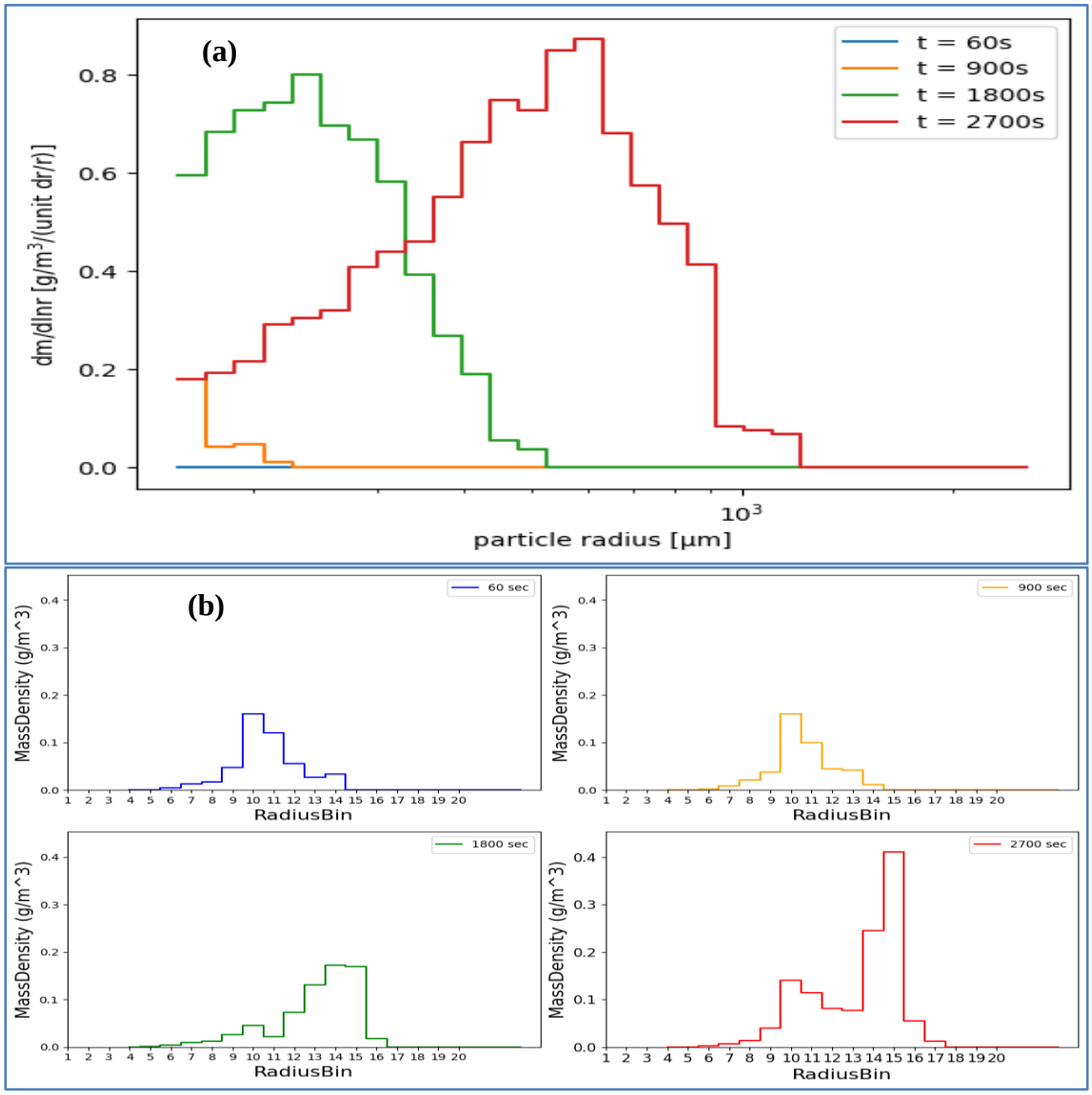

Fig. 5 (a&b) (a) Temporal evolution of droplets of Disdrometer size bin (156.5-2800.25) micrometer by PySDM. (b) Temporal evolution of mass density of droplets through the actual event measured by Disdrometer for rain rate > 10 mm/h

This phenomenon is additionally represented through mathematical modeling using the Gaussian equation which is accurately approximated shown in Fig. 3.

$$f(x) = a_1\, exp\left(-\left(\frac{(x-b_1)}{c_1}\right)^2\right) + a_2\, exp\left(-\left(\frac{(x-b_2)}{c_2}\right)^2\right) \quad (5)$$

$a_1 = 0.58$, $a_2 = 0.31$, $b_1 = 51.5$, $b_2 = 63.1$, $c_1 = 8.05$, and $c_2 = 14.6$.

where a_1 and a_2 are the amplitudes or heights of the two Gaussian components; b_1 and b_2 represent the means or centers of the two Gaussian components; c_1 and c_2 represents the standard deviations that control the widths of the two components (Hossain et al.,2014; Seshadri V. (2012)).

The efficiency of coalescence is intricately linked to droplet size, a relationship vividly portrayed in Fig. 3 and Fig. 4a. Notably, as the size bin increases, the commencement of coalescence within each bin is delayed, suggesting an earlier onset for smaller droplets compared to their larger counterparts. This phenomenon stems from the inherent characteristics of larger droplets, which possess a higher surface area-to-volume ratio, leading to increased drag forces and consequently a prolonged time to attain terminal velocity (Bowen (1950) and Twomey (1966)). Despite this delay, once terminal velocity is reached, coalescence unfolds more rapidly for larger droplets, as evidenced by Fig. 3b, where coalescence concludes sooner for this group. This indicates a greater inclination for coalescence among larger droplets.

The relationship between droplet size and the time it takes to reach peak mass density is shown in Fig. 4b. The maximum density attained by droplets varies between$(0.70 \sim 0.78) g/m^3$.

In the size range of Bin13-Bin15, spanning from 1220.5 to 1692.5 mm, droplets display a transient behavior, indicating a swift passage through this range without prolonged retention. This transience primarily arises from coalescence, where droplets merge and subsequently migrate to other size bins. Consequently, Bin13-Bin15 serves as a zone where droplets swiftly traverse, contributing to its transient nature within the broader dynamics of droplet distribution and density. Conversely, beyond bin 15, larger droplets demonstrate stability, characterized by a higher maximum density across all bins. This acceleration is attributed to the heightened propensity for coalescence among larger droplets.

Ground observations of rain droplets exhibit a pattern that resembles a Gaussian distribution, particularly evident within a short duration of 1800 seconds, as illustrated in Fig. 5. However, it's important to note that variations can occur due to the involvement of other atmospheric dynamics or external factors. These factors may introduce deviations from the ideal Gaussian distribution, leading to observed variations in the distribution of rain droplets over time.

4. Conclusions

In conclusion, our research unveils the interplay of factors influencing droplet coalescence and its consequences for rain droplet distribution. By examining ground observations and employing mathematical models, we deciphered significant insights into droplet behavior over time. Foremost among our discoveries is the pivotal role of droplet size in determining coalescence efficiency, with larger droplets exhibiting distinct dynamics compared to smaller ones. These findings deepen our understanding of precipitation processes and highlight the need for comprehensive consideration of various factors, including atmospheric conditions and external influences. Our study not only advances scientific understanding but also holds practical implications for weather prediction, hydrological modeling, and climate research. Through continued exploration of these phenomena, we aim to refine our understanding of precipitation dynamics and enhance our ability to forecast and manage water resources effectively.

Future research will focus on incorporating additional atmospheric processes, such as turbulence and evaporation, to refine the model. Comparing results with observational data from multiple geographical regions will help validate findings and improve the accuracy of rainfall estimation.

Acknowledgment

The authors express sincere gratitude to the Director, of Space Applications Centre (SAC), ISRO Ahmedabad, for his guidance and support. A part of the research was carried out under the ISRO-SMART Research Initiative Program.

Authors' Statement

The authors declare no conflicts of interest related to this research.

Competing interest

The authors affirm that they have no competing interests related to this research.

Author contribution

Nita H. Shah: Resources. (*email: nitahshah@gmail.com*). Jyoti Chahal: Conceptualization, Methodology, Implementation Idea and Writing-original draft preparation(*email: jyotichahall.jc@gmail.com*). Bipasha Paul Shukla: Conceptualization, Writing—review and editing and Resources (*email :bipasha@sac.isro.gov.in*).

Disclaimer: The contents and views expressed in this research paper/article are the views of the authors and do not necessarily reflect the views of the organizations they belong to.

References

Bartholomew, M. J., 2009, "Disdrometer and tipping bucket rain gauge handbook. *ARM Climate Research Facility*. https://doi.org/10.2172/1019411 .

Bartlett, J. T. (1966). The growth of cloud droplets by coalescence. *Quarterly Journal of the Royal Meteorological Society*, *92*(391), 93-104. https://doi.org/10.1002/qj.49709239108.

Bartman, P., & Arabas, S. (2021). On the design of Monte-Carlo particle coagulation solver interface: A CPU/GPU super-droplet method case study with PySDM. In *Computational Science–ICCS 2021: 21st International Conference, Krakow, Poland, June 16–18, 2021, Proceedings, Part II 21* (pp. 16-30). Springer International Publishing. https://www.doi.org/10.1007/978-3-030-77964-1_2.

Bartman, P., Bulenok, O., Górski, K., Jaruga, A., Łazarski, G., Olesik, M., ... & Arabas, S. (2021). PySDM v1: particle-based cloud modelling package for warm-rain microphysics and aqueous chemistry. *arXiv preprint arXiv:2103.17238*. https://doi.org/10.48550/arXiv.2103.17238

Beard, K. V., & Ochs III, H. T. (1993). Warm-rain initiation: An overview of microphysical mechanisms. *Journal of Applied*

Meteorology and Climatology, *32*(4), 608-625. https://doi.org/10.1175/1520-0450(1993)032.

Bowen, E. G. (1950). The formation of rain by coalescence. *Australian Journal of Chemistry*, *3*(2), 193-213. https://doi.org/10.1071/CH9500193?urlappend=%3Futm_source%3Dresearchgate.net%26utm_medium%3Darticle

Gebauer, F., Villwock, J., Kraume, M. and Bart, H.J., 2016, "Detailed Analysis of Single Drop Coalescence—Influence of Ions on Film Drainage and Coalescence Time", Chemical Engineering Research and Design, 115, pp. 282–291, https://doi.org/10.1016/j.cherd.2016.08.014

Gillespie, D. T. (1972). The stochastic coalescence model for cloud droplet growth. *Journal of Atmospheric Sciences*, *29*(8), 1496-1510. https://doi.org/10.1175/1520-0469(1972)029%3C1496:TSCMFC%3E2.0.CO;2.

Hossain, J., Sharma, S., & Kishore, V. V. N. (2014). Multi-peak Gaussian fit applicability to wind speed distribution. *Renewable and Sustainable Energy Reviews*, *34*, 483-490. https://doi.org/10.1016/j.rser.2014.03.026

Kamp, J. and Kraume, M., 2016, "From Single Drop Coalescence to Droplet Swarms – Scale-up Considering the Influence of Collision Velocity and Drop Size on Coalescence Probability", *Chemical Engineering Science*, **156**, pp. 162–177, https://doi.org/10.1016/j.ces.2016.08.028

Knight, C. A., Vivekanandan, J., & Lasher-Trapp, S. G. (2002). First radar echoes and the early ZDR history of Florida cumulus. *Journal of the atmospheric sciences*, *59*(9), 1454-1472. https://doi.org/10.1175/1520-0469(2002)059%3C1454:FREATE%3E2.0.CO;2

Ko, G. H., & Ryou, H. S. (2005). Modeling of droplet collision-induced breakup process. *International Journal of Multiphase Flow*, *31*(6), 723-738. https://ui.adsabs.harvard.edu/link_gateway/2005IJMF...31..723K/doi:10.1016/j.ijmultiphaseflow.2005.02.004

Kopriwa, N., Buchbender, F., Ayesterán, J., Kalem, M., & Pfennig, A. (2012). A critical review of the application of drop-population balances for the design of solvent extraction columns: I. Concept of solving drop-population balances and modelling breakage and coalescence. *Solvent Extraction and Ion Exchange*, *30*(7), 683-723. https://doi.org/10.1080/07366299.2012.700598

Kumar, U., & Sharma, N. Advancements in Deep Neural Networks for Weather Prediction: A Transformative Approach. https://www.researchgate.net/publication/388734740_Advancements_in_Deep_Neural_Networks_for_Weather_Prediction_A_Transformative_Approach

Lau, K. M., & Wu, H. T. (2003). Warm rain processes over tropical oceans and climate implications. *Geophysical Research Letters*, 30(24). https://doi.org/10.1029/2003GL018567

Ma, Z., Mei, G., & Xu, N. (2024). Generative deep learning for data generation in natural hazard analysis: motivations, advances, challenges, and opportunities. *Artificial Intelligence Review*, *57*(6), 160. https://doi.org/10.1007/s10462-024-10764-9

Morrison, H., van Lier-Walqui, M., Fridlind, A. M., Grabowski, W. W., Harrington, J. Y., Hoose, C., & Xue, L. (2020). Confronting the challenge of modeling cloud and precipitation microphysics. *Journal of advances in modeling earth systems*, *12*(8), e2019MS001689. https://doi.org/10.1029/2019MS001689

Northrop, P. J. (2024). Stochastic models of rainfall. *Annual Review of Statistics and Its Application*, *11*. https://doi.org/10.1146/annurev-statistics-040622-023838

Onof, C., & Arnbjerg-Nielsen, K. (2009). Quantification of anticipated future changes in high resolution design rainfall for urban areas. *Atmospheric research*, *92*(3), 350-363. https://doi.org/10.1016/j.atmosres.2009.01.014

Pruppacher, H. R., Klett, J. D., & Wang, P. K. (1998). Microphysics of clouds and precipitation. https://doi.org/10.1080/02786829808965531

S. Shima; K. Kusano; A. Kawano; T. Sugiyama; S. Kawahara (2009). The super-droplet method for the numerical simulation of clouds and precipitation: a particle-based and probabilistic microphysics model coupled with a non-hydrostatic model., 135(642), 1307–1320. https://doi.org/10.1002/qj.441

Seshadri, V. (2012). *The inverse Gaussian distribution: statistical theory and applications* (Vol. 137). Springer Science & Business Media. https://doi.org/10.1007/978-1-4612-1456-4

Shankar, A., Kumar, A., & Sinha, V. (2024). Machine Learning approach in the prediction of Fog: An Early Warning System. *MAUSAM*, *75*(4), 1039-1050. https://doi.org/10.54302/mausam.v75i4.5919

Seifert, A., Khain, A., Blahak, U., & Beheng, K. D. (2005). Possible effects of collisional breakup on mixed-phase deep convection simulated by a spectral (bin) cloud model. *Journal of the atmospheric sciences*, *62*(6), 1917-1931. https://doi.org/10.1175/JAS3432.1

Smoluchowski, M. V. (1918). Versuch einer mathematischen Theorie der Koagulationskinetik kolloider Lösungen. *Zeitschrift für physikalische Chemie*, *92*(1), 129-168. https://doi.org/10.1515/zpch-1918-9209

Szumowski, M. J., Rauber, R. M., Ochs, H. T., & Miller, L. J. (1997). The microphysical structure and evolution of Hawaiian rainband clouds. Part I: Radar observations of rainbands containing high reflectivity cores. *Journal of the atmospheric sciences*, *54*(3), 369-385. https://doi.org/10.1175/1520-0469(1998)055%3C0208:TMSAEO%3E2.0.CO;2

Telford, J. W. (1955). A new aspect of coalescence theory. *Journal of Atmospheric Sciences*, *12*(5), 436-444. https://doi.org/10.1175/1520-0469(1955)012%3C0436:ANAOCT%3E2.0.CO;2

Twomey, S. (1966). Computations of rain formation by coalescence. *Journal of Atmospheric Sciences*, *23*(4), 405-411. https://doi.org/10.1175/1520-0469(1955)012%3C0436:ANAOCT%3E2.0.CO;2

Wang, L. P., Xue, Y., Ayala, O., & Grabowski, W. W. (2006). Effects of stochastic coalescence and air turbulence on the size distribution of cloud droplets. *Atmospheric research*, *82*(1-2), 416-432. https://doi.org/10.1016/j.atmosres.2005.12.011

Wu, J., 2004, *Some Properties of the Gaussian Distribution*, Technical Report, GVU Center and College of Computing, Georgia Institute of Technology, April 2004. https://www.researchgate.net/publication/2938912_Some_Properties_Of_the_Gaussian_Distribution

Yau, M. K., & Rogers, R. R. (1996). *A short course in cloud physics*. Elsevier. Zhang, H., Liu, Y., Zhang, C., & Li, N. (2025). Machine Learning Methods for Weather Forecasting: A Survey. *Atmosphere*, 16(1), 82. https://doi.org/10.3390/atmos16010082